Isotopic characterization of lifetime movement by two demersal fishes from the northeastern Gulf of Mexico

Running Head: Stable isotope values show lifetime movements

Authors:

Julie L Vecchio[1, 3]*, Jenny Ostroff[1,2], Ernst B Peebles[1]

1. College of Marine Science, University of South Florida, 830 1st St South, St. Petersburg, FL 33701
2. Present address: NOAA Fisheries, 263 13th Ave S, St. Petersburg, FL 33701
3. Present address: Florida Fish and Wildlife Research Institute, 100 8th Avenue SE, St. Petersburg, FL 33701

*jlvsses@gmail.com

ABSTRACT

An understanding of lifetime trophic changes and ontogenetic habitat shifts is essential to the preservation of marine fish species. We used carbon and nitrogen stable isotope values recorded within the laminar structure of fish eye lenses, reflecting both diet and location over time, to compare the lifetime trends of two demersal mesopredators. Tilefish, *Lopholatilus chamaeleonticeps*, is known to inhabit burrows on the outer continental shelf, which results in exceptional site fidelity. Red Grouper, *Epinephelus morio*, is spawned on the middle-to-outer continental shelf, moves to the inner shelf for the juvenile period, and returns offshore upon sexual maturity. Both species inhabit the eastern Gulf of Mexico, a region with distinctive offshore-inshore gradient in background $\delta^{13}C$ values. Within individual Tilefish (n = 36), sequences of $\delta^{13}C$ values and $\delta^{15}N$ values had strong, positive correlations with eye-lens diameter, and strong correlations between the two isotopes (mean Spearman $r = 0.86$), reflecting trophic position increase with growth and little lifetime movement. In Red Grouper, (n = 30), $\delta^{15}N$ value positively correlated with eye-lens diameter, but correlations between $\delta^{15}N$ values and $\delta^{13}C$ values were weak (mean Spearman $r = 0.29$), suggesting cross-shelf ontogenetic movements. Linear mixed model results indicated strong relationships between $\delta^{15}N$ values and $\delta^{13}C$ values in Tilefish eye lenses but no convergence in the Red Grouper model. Collectively, these results are consistent with previously established differences in the life histories of the two species, demonstrating the potential utility of eye-lens isotope records, particularly for investigating the life histories of lesser-known species.

Keywords: Stable isotopes, fish eye lenses, fish movement, $\delta^{13}C$, $\delta^{15}N$, trophic growth

1. INTRODUCTION

Many marine fish species undergo ontogenetic shifts in both location and diet, using different habitats and food resources during juvenile and adult life stages (e.g. Dahlgren E Eggleston 2001, Saul et al. 2012, Kurth et al. 2019). While an understanding of the habitat needs for each life stage is important, the extent of movement may be difficult to assess in many species. Stable isotope data can be used to interpret both species movements and trophic position (Ainsworth et al. 2015, Gruss et al. 2016). An increase in $\delta^{15}N$ values with body size is a common phenomenon among marine predators, and has been termed “trophic growth" (Wallace et al. 2014, Curtis et al. 2020, Liu et al. 2020). Within a single species, individuals often feed at higher trophic positions as they grow, resulting in trophic growth [e.g., Summer Flounder, *Paralichthys dentatus* (Buchheister & Latour 2011), Boreoatlantic Armhook Squid, *Gonatus fabricii* (Golikov et al. 2018) and Yellowfin Tuna, *Thunnus albacares* (Graham et al. 2007)]. Although trophic fractionation can be variable, $\delta^{15}N$ values in marine mesopredator tissues increase by approximately 2.3 to 3.4‰ and $\delta^{13}C$ values increase by 1.9 to 2.3‰ with each trophic step (Post 2002, McCutchan et al. 2003, Mohan et al. 2016, Eddy 2019). Tissue $\delta^{13}C$ values can be useful for indicating basal-resource dependence (Fry & Wainright 1991, Dance et al. 2018). The $\delta^{13}C$ values of subtropical marine phytoplankton have been found to be between 3.7 and 6‰ more negative than benthic primary producers (Moncreiff & Sullivan 2001, Grippo et al. 2011, Dance et al. 2018).

One factor that complicates the interpretation of individual isotopic composition bulk tissues for trophic position and basal-resource dependence in marine consumers is geographic variation in isotopic baselines. Spatial variation in stable isotope compositions (isoscapes) have been established for a number of marine regions, and these trends are reflected in the tissues of

predators moving through these areas (MacKenzie et al. 2011, Simpson et al. 2019, Trueman et al. 2019). Whereas changes in trophic position will result in changes to isotope values over time, baseline isotope values can have a similar effect on the isotopic composition of tissues assimilated during movement. For example, if a fish were to remain stationary while increasing trophic position during life, then both $\delta^{15}N$ values and $\delta^{13}C$ values would be expected to increase concomitantly as a function of positive trophic fractionation. Based on trophic discrimination factors for each isotope, the average slope of this relationship would be expected to range from 1.0 to 1.7 in marine mesopredators (Post 2002, McCutchan et al. 2003, McMahon et al. 2010). In contrast, if the baseline values of the isotopes of interest ($\delta^{15}N$ and $\delta^{13}C$, in this case) trend in different geographic directions and the fish has moved across these opposing trends, then the consistent linear relationship between the isotope values would be degraded or lost.

During organismal growth and cell maintenance, new isotopic information is continuously incorporated into various tissue types, often at distinct rates (Sweeting et al. 2005, Buchheister & Latour 2010, Heady & Moore 2013). Internal eye-lens layers (laminae) experience little or no turnover and function as a conservative record of the isotopic histories within each individual (Wallace et al. 2014, Nielsen et al. 2016, Simpson et al. 2019, Curtis et al. 2020). Peebles and Hollander (2020) provide a review of fish eye-lens physiology as it relates to stable isotopes. In short, the record-keeping behavior of eye lenses arises from lifetime conservation of optical proteins called *crystallins*. New protein synthesis within individual cells is not possible after cell formation and the subsequent apoptosis (removal) of cellular organelles, which improves the optical properties of the cells (Lynnerup et al. 2008, Rinyu et al. 2019). This selective apoptosis results in preservation of the original organic material within successively created laminae (Nicol 1989, Lynnerup et al. 2008, Stewart et al. 2013, Nielsen et al. 2016). A

captive diet-switch study (Granneman 2018) documented isotopic shifts within fish eye lenses that mirrored an isotopic shift in the feed, confirming that a change in diet is reflected in the fish eye-lens record.

The continental shelf offshore of Florida's Gulf of Mexico coast (West Florida Shelf) consists of gradually sloping soft sediment interspersed with limestone reefs and outcroppings (Locker et al. 2010, Hine & Locker 2011). Tilefish (*Lopholatilus chamaeleonticeps*) and Red Grouper (*Epinephelus morio*) are both large, demersal predators common in the northeastern Gulf of Mexico. Both species excavate soft sediments (Scanlon et al. 2005, Ellis et al. 2017) and associate closely with the burrows or depressions that they create (Able et al. 1982, Coleman et al. 2011, Ellis 2019, Grasty et al. 2019). Juveniles of both species consume benthic invertebrates (Brule & Canche 1993, Steimle et al. 1999) and the proportion of fish in the diet increases as individuals grow (Grimes et al. 1986, Weaver 1996). However, there are notable distinctions between the two species' life histories in the northeastern Gulf of Mexico.

Individual Tilefish create and maintain vertical burrows in clay sediments (Grossman et al. 1985, Grimes et al. 1986, Able et al. 1987) near the edge of the continental shelf. Smaller individuals are observed near smaller burrows, suggesting that they remain near the same burrow over many years (Able et al. 1982, Grimes 1983, Grimes et al. 1986, Fisher et al. 2014). Captive-reared Tilefish have been observed settling to the bottom and beginning to dig by 1.5 cm standard length (Fahay 1983). Because this species rarely consumes migratory prey (Steimle et al. 1999), $\delta^{13}C$ values and $\delta^{15}N$ values of lens protein should reflect local conditions at a single location throughout the lifespan.

Juvenile Red Grouper are found on the inner continental shelf (< 30 m depth), where they use rocky reef habitats (Bullock & Smith 1991). Adult Red Grouper maintain depressions in soft

sediment veneers overlying limestone outcrops on the middle to outer continental shelf (Coleman et al. 2010, Wall et al. 2011, Grasty et al. 2019). Tagging studies indicate most adult Red Grouper move little over a one-to-two year period (Burns & Froeschke 2012, Farmer & Ault 2014). However, recaptures of individuals that did move were in deeper water than the depth of original tagging (Moe 1969, Burns 2009, Saul et al. 2012). Based on these data and the relationship between size and capture depth, it is clear that Red Grouper use different habitats during life (Moe 1969, Johnson & Collins 1994, Gruss et al. 2017). The existence of ontogenetic habitat shifts thus distinguishes Red Grouper from Tilefish.

Baseline trends in fish tissue $\delta^{15}N$ values and $\delta^{13}C$ values on the West Florida Shelf are consistent among years, seasons, and species, allowing for the delineation of regional isoscapes (Figure 1a; Radabaugh et al. 2013; Radabaugh & Peebles 2014; Huelster 2015). Values of $\delta^{15}N$ are highest in the northwestern extreme and lowest on the southern end of the West Florida Shelf, which is consistent with high rates of riverine input to the north and elemental nitrogen fixation by diazotrophs to the south (McClelland et al. 2003, O'Connor et al. 2016). Trends in $\delta^{13}C$ values on the West Florida Shelf are orthogonal (rotated 90 degrees) to those of $\delta^{15}N$ values, with highest values in shallow, clear waters where benthic primary producers are more abundant (Radabaugh et al. 2013). Because of this orthogonal relationship, movement across these two isoscapes ($\delta^{15}N$ and $\delta^{13}C$) decouples temporal trends in $\delta^{13}C$ values and $\delta^{15}N$ values within the eye lenses of an individual fish.

Stable isotope values have been used in a variety of settings with a single species or a small group of species as models for life history and autecology (Tallamy & Pesek 1996, Holtum & Winter 2014, Ogston et al. 2016). We use profiles of eye-lens $\delta^{13}C$ values and $\delta^{15}N$ values from Tilefish and Red Grouper as models of distinct demersal mesopredator life histories within

a similar geographic region. We compare the isotopic histories of burrow-inhabiting Tilefish, which have lifelong site fidelity, with Red Grouper, which move long distances as they grow and mature. By using these two species as contrasts between a lifetime in a single location and lifetime of ontogenetic movement, we can use lifetime isotopic patterns to interpret movement of other species living in regions with similar isotopic contrasts, including species for which gaps exist in our understanding of life history.

2. MATERIALS AND METHODS

2.1 Material collection and preparation

We obtained 36 adult Tilefish from the University of South Florida's benthic longline surveys (Murawski et al. 2018) and 30 Red Grouper from the Southeast Area Monitoring and Assessment Program's (SEAMAP) groundfish trawl surveys (Eldridge 1988). Tilefish were collected from the northern West Florida Shelf and adjacent areas to the west (Figure 1b) in water depths of 178 to 375 m. Red Grouper were collected from the northern and central West Florida Shelf (Figure 1b) in water depths of 10 to 40 m. Tilefish were measured to the nearest cm fork length (FL), dissected, and sexed macroscopically at sea. Red Grouper were measured to the nearest mm FL and dissected at sea but were not sexed due to the difficulty of macroscopic sex designation in the species (Lowerre-Barbieri et al. 2014). All specimens were beyond the length at 50% maturity (SEDAR 2011, Lombardi-Carlson 2014). Red Grouper is known to be protogynous, with 50% transition to male at 743 mm FL and 11.5 y (Lowerre-Barbieri et al. 2014). Otoliths were cleaned of tissue before storing dry at room temperature, and whole eyes were frozen at -20°C until analysis.

Sagittal otoliths were aged by counting annuli under transmitted light microscopy using an Olympus SZX12 zoom stereomicroscope. Each species was aged according to the method employed by the Florida Fish and Wildlife Conservation Commission's Age and Growth Lab, which assisted on this project. Tilefish otoliths were thin-sectioned, attached to a microscope slide, and annuli were counted (Lombardi-Carlson & Andrews 2015). Red Grouper otoliths were aged whole in a water-filled petri dish (Johnson & Collins 1994). Data on age and length were combined to confirm maturity status (Tables S1 and S2; SEDAR 2011, Lombardi-Carlson 2014).

We dissected and processed eye lenses according to Wallace et al. (2014) immediately prior to isotope analysis. We thawed whole eyes individually, removed the lens from the lens capsule, placed each lens on a glass petri dish, and measured eye-lens diameter (ELD) to the nearest 0.05 mm using an ocular micrometer in an Olympus SZX12 zoom stereomicroscope at 10x magnification. We delaminated each lens using two fine-tipped forceps under 10x-50x magnification and recorded the ELD after removal of each lamina. We identified each lamina based on its diameter midpoint (midpoint between successive ELDs). The lens core (< 1 mm diameter) was the final tissue in the analyzed series. De-ionized water was used sparingly for Tilefish eye-lens delamination, but Red Grouper eye lenses were submerged in water for delamination. The two methods have been shown to result in comparable isotopic values (Meath et al. 2019). Laminar material became desiccated in <1 h at 25 °C.

2.2 Isotope analysis

For isotope analysis, we weighed 200-600 µg of eye-lens material from each lamina to the nearest µg on a Mettler-Toledo precision microbalance. We used a Carlo-Erba NA2500 Series II Elemental Analyzer (EA) combustion furnace coupled to a continuous-flow ThermoFinnigan Delta+XL isotope ratio mass spectrometer (IRMS) to measure $^{13}C/^{12}C$ and

$^{15}N/^{14}N$ and C:N in duplicate at the University of South Florida College of Marine Science in St. Petersburg, Florida. Calibration standards were NIST 8573 (-26.39 ± 0.09‰ and -4.52 ± 0.12‰ for $\delta^{13}C$ and $\delta^{15}N$ values respectively) and NIST 8574 L-glutamic acid (+37.63 ± 0.10‰ and +47.57 ± 0.22‰ for $\delta^{13}C$ and $\delta^{15}N$ values respectively) standard reference materials. Results are presented in delta notation (δ, in ‰) relative to international standards Vienna Pee Dee Belemnite (VPDB) for carbon and air for nitrogen

$$\delta X = \left(\frac{R_{sample}}{R_{standard}} - 1\right) \times 1000$$

where X is either ^{13}C or ^{15}N and R is the isotopic ratio of interest (e.g. ^{13}C:^{12}C). Analytical precision, obtained by replicate measurements of NIST 1577b bovine liver, was ± 0.20‰ for $\delta^{13}C$ values and ± 0.30‰ for $\delta^{15}N$ values (maximum standard deviations of n = 300 replicates).

2.3.1 Eye-lens isotope data analysis

All data analyses were conducted in R statistical software version 3.6.1 (R Core Team 2019). Eye-lens isotope profiles represent changes in the eye-lens $\delta^{13}C$ values and $\delta^{15}N$ values throughout each fish's lifetime with innermost lamina representing the youngest age (postlarval period) and outermost lamina representing age at capture. Eye lenses do not contain known age-marks. Therefore, we used the best-fit regression to relate eye-lens diameter to FL for each species. For Tilefish, we used the linear regression $FL(cm) = 6.03 \times ELD\ (mm)$; F = 1220, R^2 = 0.97, $p < 0.001$ (n = 36, FL range = 48–99 cm). The regression was constructed using maximum eye-lens diameter and FL for the individuals used for this study. For Red Grouper, we used the logarithmic regression $FL\ (cm) = e^{(e+0.21 \times ELD)}$; F = 510, R^2 = 0.84, $p < 0.01$ (n = 99, FL range = 4.4–80.5 cm). The regression was constructed using the individuals from the current study as well as 69 juveniles ranging from 4.4 to 30.0 cm FL.

We calculated mean and standard error for the eye-lens $\delta^{13}C$ values and $\delta^{15}N$ values of each species. Subsequently, we used routines PERMDISPER and PERMANOVA in R (package Vegan, Oksanen et al. 219) to compare $\delta^{13}C$ values to $\delta^{15}N$ values from the 468 individual Tilefish eye-lens laminae with the 406 Red Grouper eye-lens laminae.

For each species, we measured the fit of a logarithmic curve $\delta X = a + b \times \ln(ELD)$, where a is the parameter controlling the curve location on the y-axis and b is the parameter controlling curve shape. This model was chosen as a version of growth equations commonly used in fish (von Bertalanffy 1938, Ricker 1975). Regression trends can be attributed to changes in trophic position with somatic growth. Substantial deviation from this curve can be attributed to movement across the background isoscape or change in basal-resource dependence. We used routine lmer in package LME4 (Bates et al. 2015) to construct linear mixed effects models comparing $\delta^{13}C$ values to $\delta^{15}N$ values in each species, using individual fish as a random effect. We used the permanova.lmer function in package Predictmeans (Luo et al. 2020) to compute a permuted p-value for the overall model in each species.

2.3.2 Isotope interpretations: Movement vs. trophic-position increase for individual fish

We used a series of correlations to distinguish between the influence of changing trophic position and movement within individual eye-lens isotope profiles. We identified all possible isotopic outcomes that would be associated with different combinations of geographic movement (Radabaugh & Peebles 2014) or trophic position increase with growth (Fry 2006, Wallace et al. 2014) at the individual level (Figure 2). In Figure 2, gray-shaded cells represent these trends (positive, negative, or neutral), as indicated by significant departures of lifetime regression slopes from zero. The potential geographic and trophic explanations for these trends are presented in unshaded cells. For example, an individual may have a positive lifetime trend (+,

shaded gray) in $\delta^{15}N$ values or $\delta^{13}C$ values for three reasons: (1) it moved in a positive direction along a baseline isotopic gradient while increasing its trophic position, (2) it increased its trophic position without substantial movement, or (3) it moved in a positive direction along a baseline isotopic gradient without substantially changing its trophic position.

In addition to these lifetime trends, we considered another suite of relationships [via Spearman correlation (r_s)] that provided additional information; the conceptual outcomes of these are presented in Table 1 (which is analogous to Figure 2 except based on correlation). Specifically,

1) we correlated $\delta^{15}N$ values with ELD within individual eye-lens profiles to determine whether trophic growth or movement along the $\delta^{15}N$-value gradient had occurred (Hansson et al. 1997),
2) we correlated $\delta^{13}C$ values with ELD within individual eye-lens profiles to determine whether movement along the $\delta^{13}C$ baseline had occurred or if basal-resource dependence had changed (Fry & Wainright 1991, Radabaugh & Peebles 2014), and
3) we correlated $\delta^{13}C$ values with $\delta^{15}N$ values within individual eye-lens profiles to represent site fidelity, with strong correlations indicating high site fidelity during life (McCutchan et al. 2003, Meath et al. 2019).

Individuals with strong correlations in all three tests were interpreted as having experienced trophic growth with little to no geographic movement, eliminating one of two possible interpretations for the isotope profiles in Figure 2. We acknowledge that this approach is subject to both Type I and Type II errors but represents one possible way of moving from a population-level to an individual-level interpretation.

3. RESULTS

3.1 Biological and isotopic comparisons between species

Red Grouper ranged from 29.2 to 78.1 cm FL and 2 to 10 years, with one fish unaged. Tilefish ranged from 48 to 99 cm fork length (FL) and 8 to 20 years, with four fish unaged (Tables S1 and S2). Multiple linear regression (R Core Team 2019) did not detect a relationship between FL and capture depth or capture latitude for either species (Tilefish: $F_{2,33} = 2.38$, $R^2 = 0.13$, $p = 0.108$; Red Grouper: $F_{2,26} = 0.06$, $R^2 = 0.01$, $p = 0.95$).

Multivariate isotope location was significantly different between the two species ($F = 923.56$, $R^2 = 0.49$, $p < 0.001$; Figure 3) as was multivariate dispersion ($F = 14.60$, $p < 0.001$). Tilefish mean (± SE) eye-lens $\delta^{15}N$ values and $\delta^{13}C$ values were 12.97 ± 0.07 and -17.49 ± 0.04 respectively. Red Grouper mean (± SE) eye-lens $\delta^{15}N$ values and $\delta^{13}C$ values were 9.46 ± 0.06 and -16.49 ± 0.06 respectively. In both Red Grouper and Tilefish, ELD had positive, logarithmic relationships with $\delta^{13}C$ values and $\delta^{15}N$ values (Table 2, Figure 4). Fits were over $R^2 = 0.5$ between ELD and Tilefish $\delta^{13}C$ values, Tilefish $\delta^{15}N$ values, and Red Grouper $\delta^{15}N$ values. However, Red Grouper $\delta^{13}C$ values were not well represented by this model ($R^2 = 0.12$; Table 2, Figure 4). We found a positive linear relationship between Tilefish $\delta^{15}N$ values and $\delta^{13}C$ values in the form $\delta^{15}N = a + b^* \delta^{13}C$ (Table 3, Figure 5a). However, the linear mixed model for the relationship between $\delta^{15}N$ values and $\delta^{13}C$ values in Red Grouper failed to converge (Figure 5b).

3.2 Relationships between ELD, $\delta^{13}C$ values, and $\delta^{15}N$ values at the individual level

Individual Red Grouper eye-lens $\delta^{15}N$ values increased as the fish grew (mean $\Delta\delta^{15}N$ ± SE = 3.60 ± 0.20‰). Despite Red Grouper average increases in $\delta^{13}C$ values over the lifetime (mean $\Delta\delta^{13}C$ ± SE = 1.93 ± 0.22‰), visual inspection indicated that most profiles peaked near 2 mm ELD (Figure S1). The mean correlation between $\delta^{15}N$ value and ELD was $r_s = 0.75$ ($p <$

0.001) and the mean correlation between $\delta^{13}C$ value and ELD was $r_s = 0.29$ ($p = 0.50$). Correlations between $\delta^{15}N$ value and ELD were positive and significant in all individuals while $\delta^{13}C$ value and ELD were positive and significant for 10 of 30 fish (Table S1). Profiles of eye-lens $\delta^{15}N$ value as a function of $\delta^{13}C$ value for each individual were highly variable in both slope and direction (Figure S3). Five of 30 Red Grouper appeared to increase their trophic positions while remaining stationary and continuing to depend on similar basal resources, while the remainder appeared to move substantial distances across isotopic gradients and/or change their basal-resource dependence (Table S1).

In each individual Tilefish eye lens, there was an increase in $\delta^{13}C$ values and $\delta^{15}N$ values during life. Lifetime $\Delta\delta^{13}C$ value was 2.50 ± 0.12‰ (mean ± SE) and lifetime $\Delta\delta^{15}N$ value was 4.67 ± 0.17‰ (mean ± SE; Figure S2). Average Tilefish correlation between $\delta^{15}N$ value and ELD was $r_s = 0.80$ ($p < 0.001$), and correlation between $\delta^{13}C$ value and ELD was $r_s = 0.70$ ($p <$ .0001). Average correlation between $\delta^{13}C$ values and $\delta^{15}N$ values was $r_s = 0.86$ ($p < 0.001$; Table S2) within individual fish. Nearly all (35 out of 36) Tilefish appeared to increase their trophic positions during life while remaining in the same location and feeding within the same basal-resource regime. Only the smallest Tilefish was suspected of a change in basal-resource dependence based on these rules (Table S2).

4. DISCUSSION

We used the isotope profiles reconstructed from fish eye lenses as a novel approach for detecting ontogenetic habitat shifts. We took advantage of the spatially decoupled isoscapes of fish tissue $\delta^{13}C$ values and $\delta^{15}N$ values in the eastern Gulf of Mexico (Figure 1a) to interpret eye-lens isotope profiles as movement on a lifetime scale. We used Tilefish, a lifelong burrow-

inhabiting species, as a model of a stationary species. We contrasted the isotope profiles in these eye lenses with those of Red Grouper, which is known to move inshore and then offshore across the West Florida Shelf with changing ontogeny. The shapes of eye-lens isotope profiles and correlations between isotopes, coupled with the orthogonal isotopic background, suggest similar patterns of movement could be detected for any species living in an area with a similarly decoupled isotopic backgrounds.

Differences in overall isotopic values between Tilefish and Red Grouper (Figure 3) follow background trends in $\delta^{13}C$ values and $\delta^{15}N$ values for the region (Figure 1a). Tilefish in the Gulf of Mexico inhabit a narrow geographic range in areas that have a steep depth gradient (Steimle et al. 1999, Pierdomenico et al. 2015). All Tilefish in this study were collected in 178 to 375 m depths, with little cross-shelf distribution (Figure 1b), which is reflected in their relatively high, tightly grouped $\delta^{13}C$ values and $\delta^{15}N$ values. Red Grouper occur on patchy reef habitats of the West Florida Shelf (Moe 1969, Coleman et al. 2010), usually in waters less than 100 m depth (SEDAR 2015). All Red Grouper in this study were collected in 10 to 40 m to the east and southeast of Tilefish collections (Figure 1b). The wide range of eye-lens $\delta^{13}C$ values in Red Grouper reflect cross-shelf movement over time, and the low eye-lens $\delta^{15}N$ values reflect their reliance on more southern habitats than Tilefish (Figures 1b and 3).

In order to enhance interpretation and broaden applications of eye lens stable isotope data, we developed an approach that established generalized rules of interpretation (Table 1 and Figure 2). We first segregated the potential effects of trophic change and movement on fish eye-lens isotope values, and then recombined these effects to simulate all possible isotopic outcomes (Figure 2), similar to Meath et al. (2019). We expanded this exercise to include all possible correlations between isotope values and fish length, using ELD as a proxy (Table 1).

We observed the lowest $\delta^{15}N$ values during the earliest phases of exogenous feeding in both species, which is consistent with previous eye-lens isotope findings (Wallace et al. 2014, Quaeck-Davies et al. 2018, Simpson et al. 2019). In both species, $\delta^{15}N$ values fit a logarithmic function of ELD (Table 2, Figure 4), with isotope values increasing at a faster rate during early life, similar to trends in fish body length (Juanes 2016) and in agreement with a recent fish eye-lens isotope study (Curtis et al. 2020). One mechanism for trophic increase with body growth is the addition of larger prey to the available prey pool as gape limitation decreases (Dalponti et al. 2018). In addition, large individuals at higher trophic positions, which are capable of substituting different trophic pathways into their diets, reduce vulnerability to basal-resource instability (MacKenzie et al. 2012, Burghart et al. 2013, Dalponti et al. 2018).

At the individual level, Spearman rank correlations were significant between $\delta^{15}N$ values and ELD in all 36 individual Tilefish and in 27 of 30 Red Grouper (90%). There was no significant correlation between $\delta^{15}N$ value and ELD in three Red Grouper, suggesting that some individuals either did not increase their trophic positions or they moved far enough (southward) to isotopically negate the increase in $\delta^{15}N$ value expected from trophic growth. Red Grouper tagging studies have shown that substantial movement is uncommon for adults over a one-to-two-year time period (Burns & Froeschke 2012), but some individuals have been shown to move > 50 km southward, a distance sufficient to offset the $\delta^{15}N$ value increase from trophic growth on the West Florida Shelf (Burns 2009).

The logarithmic model relating Tilefish eye-lens $\delta^{13}C$ value to ELD fit the data well, as did Spearman rank correlations between $\delta^{13}C$ value and ELD for individuals, suggesting consistent growth with little movement over time (Table 2, Figure 4). The Red Grouper logarithmic model did not have a tight fit (Table 2, Figure 4), and $\delta^{13}C$ values did not correlate

significantly with ELD in most individuals. Many of the non-significant relationships were due to peaks in the $\delta^{13}C$ values during early life (Figure S1), potentially revealing ontogenetic changes in habitat use and/or basal-resource dependence by moving inshore and then back offshore before sexual maturity (Keough et al. 1998, Araujo et al. 2007, Ellis et al. 2014).

Trophic fractionation without concurrent movement over time couples $\delta^{13}C$ values to $\delta^{15}N$ values in a lifetime record such as eye lenses. Both $\delta^{13}C$ values and $\delta^{15}N$ values increase together as trophic position changes. Based on data from other marine mesopredators, the slope of this relationship would be approximately 1.0 to 1.7 (McCutchan et al. 2003, Matley et al. 2016, Eddy 2019). However, the linear relationship between tissue isotopes is disrupted if the fish move across isoscapes that are not spatially correlated with one another (i.e., the processes that control them are decoupled), as is the case in the $\delta^{13}C$ value and $\delta^{15}N$ value isoscapes on the West Florida Shelf. Thus, our proposed explanation for correlations in Tilefish eye lenses (Figure 5a, S2, S4) is increased trophic position as mouth gape increases, coupled with a lack of movement along either isoscape. Indeed, the average slope of the relationship between $\delta^{15}N$ values and $\delta^{13}C$ values was 1.5‰ in this species (Figure 5a), within the range of values expected for marine mesopredators. Whereas trophic growth can also be observed in Red Grouper eye lens $\delta^{15}N$ value profiles (Figures 4c and S2), correlations between $\delta^{13}C$ values and $\delta^{15}N$ values are weak in this species (Figure S4), and no linear relationship existed between the two isotopes (Figure 5b). Taken together, these data suggest most individual Red Grouper moved considerable distances across the $\delta^{13}C$ isoscape during their lifetimes.

The eye-lens isotope profiles observed in Tilefish and Red Grouper are consistent with available life-history and diet information for the two species. In future studies of fish eye-lens isotopes, we suggest using models to investigate changes in trophic position, basal-resource

dependence, and movement in populations as a whole, and a series of correlations to evaluate trends within individuals. In areas where $\delta^{13}C$ and $\delta^{15}N$ values are not spatially correlated, we suggest a strong correlation between $\delta^{13}C$ and $\delta^{15}N$ values in eye-lens profiles serves as an indicator of high site fidelity during trophic growth, especially when a linear relationship between the two isotope profiles has a slope between 1.0 and 1.7. In contrast, a weak correlation between the profiles of these two isotopes and a lack of linear relationship indicates ontogenetic movement across spatially variable isoscapes. Individuals with weak correlations and slopes outside this range can then be investigated for ontogenetic habitat or diet shifts using methods such as diet analysis, compound-specific stable isotope analyses of eye-lens laminae (Wallace 2019), tagging studies, or other combinations of analysis types. Our approach provides a promising alternative to subjective interpretation of lifetime isotope profiles. Taking a weight-of-evidence approach (i.e., by analyzing multiple individuals and coupling isotope data with other types of data) strengthens the interpretation. This method could be applied to species for which other life history information is lacking, providing a simple means of detecting ontogenetic movement in poorly studied species.

ACKNOWLEDGMENTS

The authors wish to recognize the important intellectual contributions made to this effort by the late David J. Hollander (University of South Florida College of Marine Science). This research was supported by the Florida RESTORE Act Centers of Excellence Program, administered by the Florida Institute of Oceanography (USF awards 4710112604 and 4710112901), and by the BP/Gulf of Mexico Research Initiative (GOMRI) via the C-IMAGE research consortium. As part of C-IMAGE, Dr. Steve Murawski (USFCMS) conducted the longline sampling with the assistance of the captain and crew of the R/V *Weatherbird II*,

operated by the Florida Institute of Oceanography, along with its scientific crew, notably Amy Wallace, Susan Snyder, Kristina Deak, and Elizabeth Herdter (all USFCMS). Laboratory assistance was provided by Catherine Bruger (Ocean Conservancy). Tilefish ages were provided by Greta Helmueller, and Red Grouper ages were provided by Mike Schram (both USFCMS). Ethan Goddard and Nico Zenzola (USFCMS) conducted the stable isotope analyses. All fish collections and tissue dissections were supported by research collecting permits and IACUC protocols at the University of South Florida. All data were published in the Gulf of Mexico Research Initiative Information and Data Cooperative (GRIIDC) website (https://data.gulfresearchinitiative.org/data/R1.x135.120:0012).

LITERATURE CITED

Able KW, Grimes CB, Cooper RA, Uzmann JR (1982) Burrow construction and behavior of tilefish, *Lopholatilus chamaeleonticeps*, in Hudson submarine canyon. Environmental Biology of Fishes 7:199-205

Able KW, Twichell DC, Grimes CB, Jones RS (1987) Tilefishs of the genus Caulolatilus construct burrows in the sea floor. Bulletin of Marine Science 40:1-10

Ainsworth CH, Schirripa MJ, Luna HNM (2015) An ATLANTIS ecosystem model for the Gulf of Mexico supporting integrated ecosystem assessment. NOAA Technical Memorandum NMFS-SEFSC-676, Vol.,US Department of Commerce, Miami, FL

Araujo MS, Bolnick DI, Machado G, Giaretta AA, dos Reis SF (2007) Using delta C-13 stable isotopes to quantify individual-level diet variation. Oecologia 152:643-654

Bates D, Mächler M, Bolker B, Walker SC (2015) Fitting linear fixed effect models using LME4. Journal of Statistical Software 67

Brule T, Canche LGR (1993) Food habits of juvenile red groupers, *Epinephelus morio* (Valenciennes, 1828) from Campeche bank, Yucatan, Mexico. Bulletin of Marine Science 52:772-779

Buchheister A, Latour RJ (2010) Turnover and fractionation of carbon and nitrogen stable isotopes in tissues of a migratory coastal predator, summer flounder (Paralichthys dentatus). Canadian Journal of Fisheries and Aquatic Sciences 67:445-461

Buchheister A, Latour RJ (2011) Trophic ecology of Summer Flounder in lower Chesapeake Bay inferred from stomach content and stable isotope analyses. Transactions of the American Fisheries Society 140:1240-1254

Bullock LH, Smith GB (1991) Seabasses (Pisces: Serranidae). Memoirs of the Hourglass Cruises 8:1-243

Burghart SE, Jones DL, Peebles EB (2013) Variation in estuarine consumer communities along an assembled eutrophication gradient: Implications for trophic instability. Estuaries and Coasts 36:951-965

Burns K (2009) Evaluation of the efficacy of the minimum size rule in the Red Grouper and Red Snapper fisheries with respect to J and circle hook mortality and barotrauma and the consequences for survival and movement. University of South Florida

Burns KM, Froeschke JT (2012) Survival of Red Grouper (*Epinephalus morio*) and red snapper (*Lutjanus campechanus*) caught on J-hooks and circle hooks in the Florida recreational and recreational-for-hire fisheries. Bulletin of Marine Science 88:633-646

Coleman FC, Koenig CC, Scanlon KM, Heppell S, Heppell S, Miller MW (2010) Benthic habitat modification through excavation by red grouper, *Epinephelus morio*, in the northeastern Gulf of Mexico. Open Fish Science Journal 3:1-15

Coleman FC, Scanlon KM, Koenig CC (2011) Groupers on the edge: shelf edge spawning habitat in and around marine reserves of the northeastern Gulf of Mexico. Professional Geographer 63:456-474

Curtis JS, Albins MA, Peebles EB, Stallings CD (2020) Stable isotope analysis of eye lenses from invasive lionfish yields record of resource use. Mar Ecol Prog Ser 637:181-197

Dahlgren CP, Eggleston DB (2001) Spatio-temporal variability in abundance, size and microhabitat associations of early juvenile Nassau grouper *Epinephelus striatus* in an off-reef nursery system. Mar Ecol Prog Ser 217:145-156

Dalponti G, Guariento RD, Caliman A (2018) Hunting high or low: body size drives trophic position among and within marine predators. Mar Ecol Prog Ser 597:39-46

Dance KM, Rooker JR, Shipley JB, Dance MA, Wells RJD (2018) Feeding ecology of fishes associated with artificial reefs in the northwest Gulf of Mexico. Plos One 13

Eddy C (2019) Trophic discrimination factors for invasive lionfish (Pterois volitans and P. miles) in Bermuda. Biological Invasions

Eldridge PJ (1988) The southeast area monitoring and assessment program (SEAMAP)- A state-federal-university program for collection, management, and dissemination of fishery-independent data and information in the southeastern United States. Marine Fisheries Review 50:29-39

Ellis GS, Herbert G, Hollander DJ (2014) Reconstructing carbon sources in a dynamic estuarine ecosystem using oyster amino acid delta C-13 values from shell and tissue. Journal of Shellfish Research 33:217-225

Ellis R (2019) Red Grouper (*Epinephelus morio*) shape faunal communities via multiple ecological pathways. Diversity 11, 89

Ellis RD, Coleman FC, Koenig CC (2017) Effects of habitat manipulation by red grouper, Epinephelus morio, on faunal communities associated with excavations in Florida Bay. Bulletin of Marine Science 93:961-983

Fahay MP (1983) Guide to the early stages of marine fishes occurring in the western north Atlantic Ocean, Cape Hatteras to the southern Scotian Shelf. Journal of Northwest Atlantic Fishery Science 4:493

Farmer NA, Ault JS (2014) Modeling coral reef fish home range movements in Dry Tortugas, Florida. The Scientific World Journal 2014:629791-629791

Fisher JAD, Frank KT, Petrie B, Leggett WC (2014) Life on the edge: environmental determinants of tilefish (Lopholatilus chamaeleonticeps) abundance since its virtual extinction in 1882. Ices Journal of Marine Science 71:2371-2378

Fry B, Wainright SC (1991) Diatom sources of C-13 rich carbon in marine food webs. Mar Ecol Prog Ser 76:149-157

Fry B (2006) Stable isotope ecology, Vol. Springer Science+Business Media, New York, MY

Golikov AV, Ceia FR, Sabirov RM, Zaripova ZI, Blicher ME, Zakharov DV, Xavier JC (2018) Ontogenetic changes in stable isotope ($\delta^{13}C$ and $\delta^{15}N$) values in squid *Gonatus fabricii* (Cephalopoda) reveal its important ecological role in the Arctic. Mar Ecol Prog Ser 606:65-78

Graham BS, Grubbs D, Holland K, Popp BN (2007) A rapid ontogenetic shift in the diet of juvenile Yellowfin Tuna from Hawaii. Mar Biol 150:647-658

Granneman JE (2018) Evaluation of trace-metal and isotopic records as techniques for tracking lifetime movement patterns in fishes. University of South Florida

Grasty S, Wall CC, Gray JW, Brizzolara J, Murawski SA (2019) Temporal persistence of Red Grouper holes and analysis of associated fish assemblages from towed camera data in the Steamboat Lumps marine protected area. Transactions of the American Fisheries Society:1-9

Grimes CB (1983) A technique for tagging deepwater fish. Fishery Bulletin 81:663-666

Grimes CB, Able KW, Jones RS (1986) Tilefish, *Lopholatilus chamaeleonticeps*, habitat, behavior and community structure in md-Atlantic and southern New England waters. Environmental Biology of Fishes 15:273-292

Grippo MA, Fleeger JW, Dubois SF, Condrey R (2011) Spatial variation in basal resources supporting benthic food webs revealed for the inner continental shelf. Limnology and Oceanography 56:841-856

Grossman GD, Harris MJ, Hightower JE (1985) The relationship between tilefish, *Lopholatilus chamaleleonticeps*, abundance and sediment composition off Georgia. Fishery Bulletin 83:443-447

Gruss A, Schirripa MJ, Chagaris D, Velez L and others (2016) Estimating natural mortality rates and simulating fishing scenarios for Gulf of Mexico red grouper (Epinephelus morio) using the ecosystem model OSMOSE-WFS. J Mar Syst 154:264-279

Gruss A, Thorson JT, Sagarese SR, Babcock EA, Karnauskas M, Walter JF, III, Drexler M (2017) Ontogenetic spatial distributions of red grouper (*Epinephelus morio*) and gag grouper (*Mycteroperca microlepis*) in the US Gulf of Mexico. Fisheries Research 193:129-142

Hansson S, Hobbie JE, Elmgren R, Larsson U, Fry B, Johansson S (1997) The stable nitrogen isotope ratio as a marker of food-web interactions and fish migration. Ecology 78:2249-2257

Heady WN, Moore JW (2013) Tissue turnover and stable isotope clocks to quantify resource shifts in anadromous rainbow trout. Oecologia 172:21-34

Hine AC, Locker SD (2011) The Florida Gulf of Mexico continental shelf—great contrasts and significant transitions. In: The Gulf of Mexico: Origin, Waters, and Marine Life

Holtum JAM, Winter K (2014) Limited photosynthetic plasticity in the leaf-succulent CAM plant Agave angustifolia grown at different temperatures. Funct Plant Biol 41:843-849

Huelster S (2015) Comparison of isotope-based biomass pathways with groundfish community structure in the eastern Gulf of Mexico. Masters thesis, University of South Florida

Johnson AG, Collins LA (1994) Age-size structure of red grouper, (*Epinephelus morio*), from the eastern Gulf of Mexico. Northeast Gulf Science 13:101-106

Juanes F (2016) A length-based approach to predator-prey relationships in marine predators. Canadian Journal of Fisheries and Aquatic Sciences 73:677-684

Keough JR, Hagley CA, Ruzycki E, Sierszen M (1998) delta C-13 composition of primary producers and role of detritus in a freshwater coastal ecosystem. Limnology and Oceanography 43:734-740

Kurth BN, Peebles E, Stallings CD (2019) Atlantic Tarpon (*Megalops atlanticus*) exhibit upper estuarine habitat dependence followed by foraging system fidelity after ontogenetic habitat shifts. Estuarine Coastal and Shelf Science

Liu BL, Xu W, Chen XJ, Huan MY, Liu N (2020) Ontogenetic shifts in trophic geography of jumbo squid, Dosidicus gigas, inferred from stable isotopes in eye lens. Fisheries Research 226

Locker SD, Armstrong RA, Battista TA, Rooney JJ, Sherman C, Zawada DG (2010) Geomorphology of mesophotic coral ecosystems: current perspectives on morphology, distribution, and mapping strategies. Coral Reefs 29:329-345

Lombardi-Carlson L (2014) Age and growth description of red grouper (*Epinephelus morio*) from the northeastern Gulf of Mexico: 1978-2013 SEDAR 42, North Charleston, SC

Lombardi-Carlson LA, Andrews AH (2015) Age estimation and lead-radium dating of golden tilefish, *Lopholatilus chamaeleonticeps*. Environmental Biology of Fishes 98:1787-1801

Lowerre-Barbieri S, Crabtree L, Switzer TS, McMichael Jr. RH (2014) Maturity, sexual transition, and spawning seasonality in the protogynous red grouper on the West Florida Shelf SEDAR 42. SEDAR42-DW-7, North Charleston, SC, p 21 pp

Luo D, Ganesh S, Koolaard J (2020) Package Predictmeans for R

Lynnerup N, Kjeldsen H, Heegaard S, Jacobsen C, Heinemeier J (2008) Radiocarbon Dating of the Human Eye Lens Crystallines Reveal Proteins without Carbon Turnover throughout Life. Plos One 3

MacKenzie KM, Palmer MR, Moore A, Ibbotson AT, Beaumont WRC, Poulter DJS, Trueman CN (2011) Locations of marine animals revealed by carbon isotopes. Scientific Reports 1

MacKenzie KM, Trueman CN, Palmer MR, Moore A, Ibbotson AT, Beaumont WRC, Davidson IC (2012) Stable isotopes reveal age-dependent trophic level and spatial segregation during adult marine feeding in populations of salmon. Ices Journal of Marine Science 69:1637-1645

Matley JK, Fisk AT, Tobin AJ, Heupel MR, Simpfendorfer CA (2016) Diet-tissue discrimination factors and turnover of carbon and nitrogen stable isotopes in tissues of an adult predatory coral reef fish, Plectropomus leopardus. Rapid Communications in Mass Spectrometry 30:29-44

McClelland JW, Holl CM, Montoya JP (2003) Relating low delta N-15 values of zooplankton to N-2-fixation in the tropical North Atlantic: insights provided by stable isotope ratios of amino acids. Deep-Sea Research Part I-Oceanographic Research Papers 50:849-861

McCutchan JH, Lewis WM, Kendall C, McGrath CC (2003) Variation in trophic shift for stable isotope ratios of carbon, nitrogen, and sulfur. Oikos 102:378-390

McMahon KW, Fogel ML, Elsdon TS, Thorrold SR (2010) Carbon isotope fractionation of amino acids in fish muscle reflects biosynthesis and isotopic routing from dietary protein. Journal of Animal Ecology 79:1132-1141

Meath B, Peebles EB, Seibel BA, Judkins H (2019) Stable isotopes in the eye lenses of *Doryteuthis plei* (Blainville 1823): exploring natal origins and migratory patterns in the eastern Gulf of Mexico. Continental Shelf Research

Moe MAJ (1969) Biology of the Red grouper *Epinephelus morio* from the eastern Gulf of Mexico Florida Department of Natural Resources Marine Research Laboratory

Professional Papers Series. Fish and Wildlife Research Institute, St. Petersburg, FL, p 1-95
Mohan JA, Smith SD, Connelly TL, Attwood ET, McClelland JW, Herzka SZ, Walther BD (2016) Tissue-specific isotope turnover and discrimination factors are affected by diet quality and lipid content in an omnivorous consumer. Journal of Experimental Marine Biology and Ecology 479:35-45
Moncreiff CA, Sullivan MJ (2001) Trophic importance of epiphytic algae in subtropical seagrass beds: evidence from multiple stable isotope analyses. Mar Ecol Prog Ser 215:93-106
Murawski SA, Peebles EB, Gracia A, Tunnell JW, Armenteros M (2018) Comparative abundance, species composition, and demographics of continental shelf fish assemblages throughout the Gulf of Mexico. Marine and Coastal Fisheries 10:325-346
Nicol JAC (1989) The eyes of fishes, Vol. Clarendon, Oxford, England
Nielsen J, Hedeholm RB, Heinemeier J, Bushnell PG and others (2016) Eye lens radiocarbon reveals centuries of longevity in the Greenland shark (*Somniosus microcephalus*). Science 353:702-704
O'Connor BS, Muller-Karger FE, Nero RW, Hu CM, Peebles EB (2016) The role of Mississippi River discharge in offshore phytoplankton blooming in the northeastern Gulf of Mexico during August 2010. Remote Sensing of Environment 173:133-144
Ogston G, Beatty SJ, Morgan DL, Pusey BJ, Lymbery AJ (2016) Living on burrowed time: Aestivating fishes in south-western Australia face extinction due to climate change. Biological Conservation 195:235-244
Oksanen J, Blanchet FG, Friendly M, Kindt R and others (2019) Vegan: community ecology package. R package version 2.5-4
Peebles EB, Hollander DJ (2020) Combining Isoscapes with Tissue-Specific Isotope Records to Recreate the Geographic Histories of Fish. In: Murawski SA, Ainsworth CH, Gilbert S, Hollander DJ, Paris CB, Schlüter M, Wetzel DL (eds) Scenarios and Responses to Future Deep Oil Spills. Springer, Cham, Switzerland, p 203-218
Pierdomenico M, Guida VG, Macelloni L, Chiocci FL and others (2015) Sedimentary facies, geomorphic features and habitat distribution at the Hudson Canyon head from AUV multibeam data. Deep-Sea Research Part Ii-Topical Studies in Oceanography 121:112-125
Post DM (2002) Using stable isotopes to estimate trophic position: Models, methods, and assumptions. Ecology 83:703-718
Quaeck-Davies K, Bendall VA, MacKenzie KM, Hetherington S, Newton J, Trueman CN (2018) Teleost and elasmobranch eye lenses as a target for life-history stable isotope analyses. PeerJ 6:26
R Core Team (2019) R: A language and environment for statistical computing. Version 3.6.1. R Foundation for Statistical Computing, Vienna, Austria
Radabaugh KR, Hollander DJ, Peebles EB (2013) Seasonal delta C-13 and delta N-15 isoscapes of fish populations along a continental shelf trophic gradient. Continental Shelf Research 68:112-122
Radabaugh KR, Peebles EB (2014) Multiple regression models of $\delta^{13}C$ and $\delta^{15}N$ for fish populations in the eastern Gulf of Mexico. Continental Shelf Research 84:158-168
Ricker WE (1975) Computation and interpretation of biological statistics of fish populations. Bulletin of the fisheries research board of Candat 191:401

Rinyu L, Janovics R, Molnar M, Kisvarday Z, Kemeny-Beke A (2019) Radiocarbon map of a bomb-peak labeled human eye. Radiocarbon

Saul S, Die D, Brooks EN, Burns K (2012) An individual-based model of ontogenetic migration in reef fish using a biased random walk. Transactions of the American Fisheries Society 141:1439-1452

Scanlon KM, Coleman FC, Koenig CC (2005) Pockmarks on the outer shelf in the northern Gulf of Mexico: Gas-release features or habitat modifications by fish? Benthic Habitats and the Effects of Fishing 41:301-312

SEDAR (2011) SEDAR 22-Gulf of Mexico Tilefish, North Chrarleston, SC

SEDAR (2015) SEDAR 42 Stock Assessment Report - Gulf of Mexico Red Grouper. Report No. 42

Simpson S, Sims D, Trueman CN (2019) Ontogenetic trends in resource partitioning and trophic geography of sympatric skates (Rajidae) inferred fromstable isotope composition across eye lenses. Mar Ecol Prog Ser 624:103-116

Steimle FW, Zetlin CA, Berrien PL, Johnson DL, Sukwoo C (1999) Essential fish habitat source document: Tilefish, *Lopholatilus chamaeleonticeps*, life history and habitat characteristics., National Marine Fisheries Servic, Woods Hole, MA

Stewart DN, Lango J, Nambiar KP, Falso MJS and others (2013) Carbon turnover in the water-soluble protein of the adult human lens. Molecular Vision 19:463-475

Sweeting CJ, Jennings S, Polunin NVC (2005) Variance in isotopic signatures as a descriptor of tissue turnover and degree of omnivory. Functional Ecology 19:777-784

Tallamy DW, Pesek JD (1996) Carbon isotopic signatures of elytra reflect larval diet in Luperine rootworms (Coleoptera: Chrysomelidae). Environ Entomol 25:1167-1172

Trueman C, Jackson AL, Chadwick K, Coombs EJ and others (2019) Combining simulation modeling and stable isotope analyses to reconstruct the last known movements of one of Nature's giants. Peerj 7:e7912

von Bertalanffy L (1938) A quantitative theory of organic growth (inquiries on growth laws. II). Human Biology 10:181-213

Wall CC, Donahue BT, Naar DF, Mann DA (2011) Spatial and temporal variability of red grouper holes within Steamboat Lumps Marine Reserve, Gulf of Mexico. Mar Ecol Prog Ser 431:243-254

Wallace AA, Hollander DJ, Peebles EB (2014) Stable isotopes in fish eye lenses as potential recorders of trophic and geographic history. Plos One 9:e108935

Wallace AA (2019) Recreating geographic and trophic histories of fish using bulk and compound-specific isotopes from eye lenses. University of South Florida

Weaver DC (1996) Feeding ecology and ecomorphology of three seabasses (Pisces: Serranidae) in the northeastern Gulf of Mexico. University of Florida

TABLES AND FIGURES

Table 1. Rules of interpretation for all possible correlation outcomes within the eye-lens isotopic profiles of individual fishes and capture location as a function of length for the species. (ELD = eye-lens diameter. Correlation = Spearman rank correlation applied to the entire lifetime eye-lens isotopic profiles for an individual fish, or species, as indicated).

1. $\delta^{15}N$ value correlation with ELD (within individuals)
1A. If $\delta^{15}N$ value negatively correlates with ELD, then individual reduced trophic position or moved against $\delta^{15}N$ gradient.
1B. If $\delta^{15}N$ value positively correlates with ELD, then individual increased trophic position or moved with $\delta^{15}N$ gradient.
1C. If $\delta^{15}N$ value does not significantly correlate with ELD, then trophic position or movement along $\delta^{15}N$ gradient were inconsistent or did not change.
2. $\delta^{13}C$ value correlation with ELD (within individuals)
2A. If $\delta^{13}C$ value negatively correlates with ELD, Then individual reduced trophic position or moved against $\delta^{13}C$ gradient.
2B. If $\delta^{13}C$ value positively correlates with ELD, then individual increased trophic position or moved with $\delta^{13}C$ gradient.
2C. If $\delta^{13}C$ value does not significantly correlate with ELD, then trophic position, basal resource, and movement were inconsistent or did not change.
3. Capture fork length (FL) correlation with relative capture location (within species)
3A. If capture length correlates (positively or negatively) with capture location, then the species tended to have directional movement.
3B. If capture length does not correlate with relative capture position, then the species tended to be stationary or moved inconsistently.
4. $\delta^{13}C$ value correlation with $\delta^{15}N$ value (within individuals)
4A. If $\delta^{13}C$ value negatively correlates with $\delta^{15}N$ value, then the individual (or its prey) moved against one isotopic gradient and with the other,
4B. If $\delta^{13}C$ value positively correlates with $\delta^{15}N$ value, then the individual remained largely stationary while increasing trophic position.
4C. If $\delta^{13}C$ value does not correlate with $\delta^{15}N$ value, then the individual (or its prey) moved inconsistently or was both stationary and did not change tro position.

Table 2. Statistics for nonlinear least-squares regression for isotopic values ($\delta^{15}N$ or $\delta^{13}C$) as a function of eye lens diameter (ELD) in both Tilefish and Red Grouper. These regressions took the form of $\delta^{15}N$ or $\delta^{13}C = a + b*\ln(ELD)$. Parameters are presented ± standard error.

Regressed with Eye-lens diameter	*n*	a (± SE)	b (± SE)	F	*p*	R^2
Tilefish $\delta^{15}N$	468	11.02 ± 0.07	1.54 ±0.05	1069	≤ 0.001	0.70
Tilefish $\delta^{13}C$	468	-18.59 ± 0.05	0.86 ± 0.04	496	≤ 0.001	0.52
Red Grouper $\delta^{15}N$	406	8.12 ± 0.07	1.28 ± 0.06	526	≤ 0.001	0.57
Red Grouper $\delta^{13}C$	406	-17.27 ± 0.11	0.68 ± 0.09	56	≤ 0.001	0.12

Table 3. Statistics for linear mixed model of $\delta^{15}N$ value as a function of $\delta^{13}C$ value in both Tilefish and Red Grouper. All regressions took the form of $\delta^{15}N = a + b*\delta^{13}C$.

Species	*n*	a (± SE)	b (± SE)	Permuted *p-value*
Tilefish	468	39.45 ± 1.05	1.51 ± 0.06	0.001
Red Grouper	406	Model did not converge		

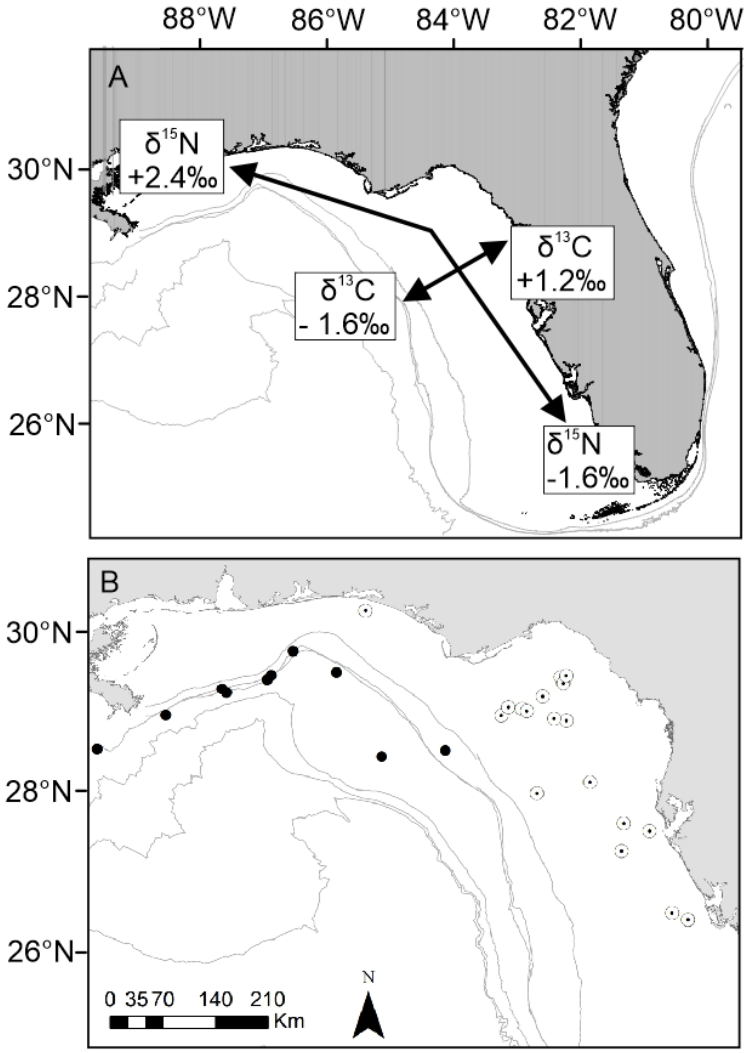

Figure 1. Region of interest, northeastern Gulf of Mexico a. Generalized background isotope (isoscape) trends (based on Radabaugh et al. 2014 and Peebles & Hollander 2020). Values in this context represent deviation from mean values; they do not represent organismal tissue values of $\delta^{13}C$ or $\delta^{15}N$. Arrows cross approximately at mean values in both isotopes. b. Collection locations for all fish in the study. Red Grouper collection locations are white symbols. Tilefish collection locations are black symbols. More than one fish was collected at several of the mapped locations. Bathymetry markings are 100, 200, 1000, 2000, and 3000 m.

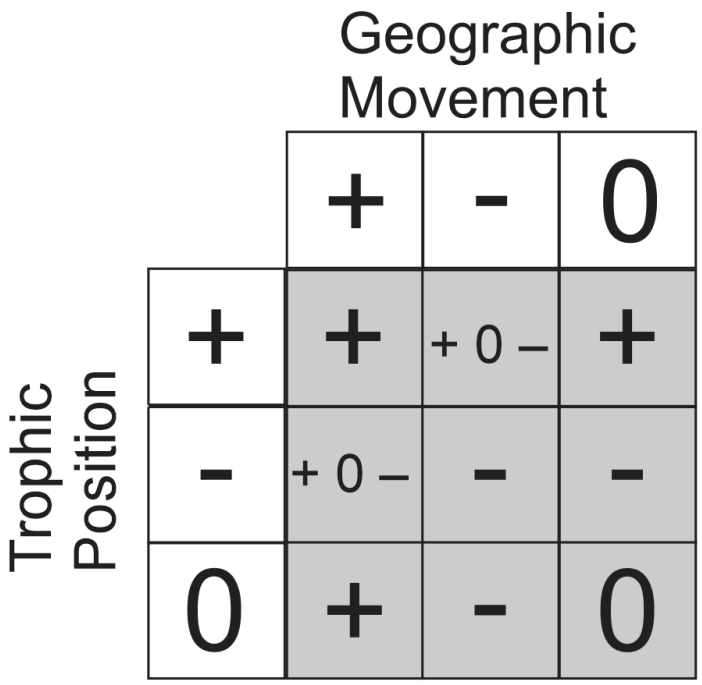

Figure 2. Interpretation of lifetime trends (regression slopes, shaded gray) in either $\delta^{13}C$ or $\delta^{15}N$ within fish eye-lenses, with trophic and geographic interpretations presented in unshaded cells. Lifetime isotopic trends (regression slopes) can be positive, negative, or neutral (+, -, or 0). Mixed inputs can result in variable observations due to differences in relative size of the change in location or trophic position.

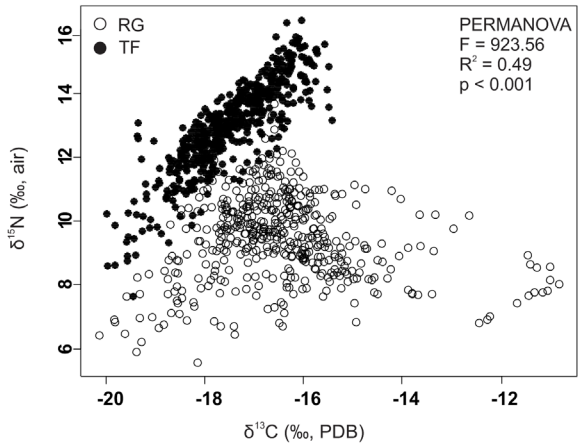

Figure 3. Isotopic distribution for all Red Grouper (RG: white symbols) and Tilefish (TF: black symbols) eye-lens laminae combined. PERMANOVA results comparing the difference in $\delta^{15}N$ and $\delta^{13}C$ by species are listed.

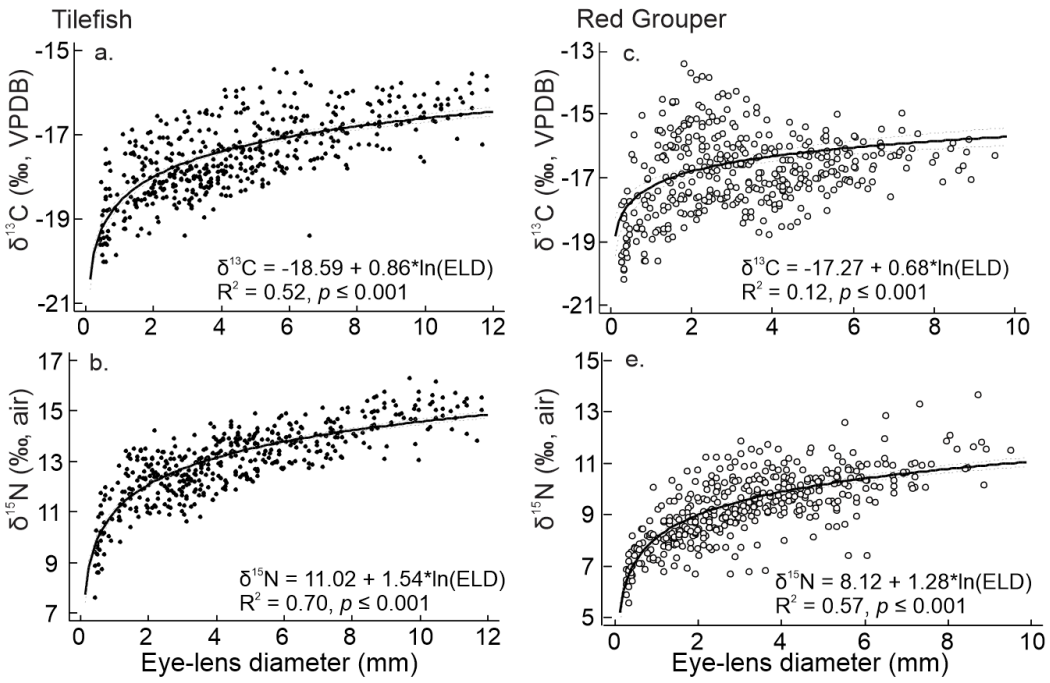

Figure 4. Non-linear regression of $\delta^{15}N$ and $\delta^{13}C$ as a function of eye-lens diameter (ELD) for both Tilefish and Red Grouper. Panels a and b are Tilefish. Panels c and d are Red Grouper.

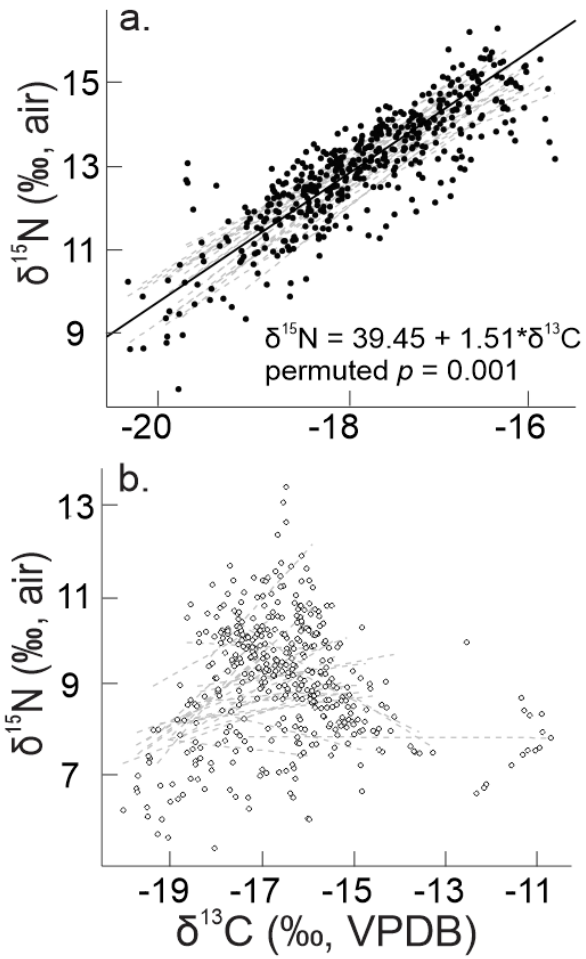

Figure 5. Linear mixed-effects model relating eye-lens $\delta^{13}C$ values to eye-lens $\delta^{15}N$ values using individual fish as a random effect within the model. The regression is in the form $\delta^{15}N = a + b*\delta^{13}C$. a. Tilefish. The equation represents the average model built using all individuals and the p-value is non-linear permuted p. b. Red Grouper. No average model is given because the model failed to converge for the species.